

Green's function variational approximation: significance of physical constraints

Krzysztof Bieniasz,^{1,2,3,*} Mona Berciu,^{2,3} and Andrzej M. Oleś^{1,4}

¹*Marian Smoluchowski Institute of Physics, Jagiellonian University, Łojasiewicza 11, PL-30348 Kraków, Poland*

²*Department of Physics and Astronomy, University of British Columbia, Vancouver, British Columbia, Canada V6T 1Z1*

³*Quantum Matter Institute, University of British Columbia, Vancouver, British Columbia, Canada V6T 1Z4*

⁴*Max-Planck-Institut für Festkörperforschung, Heisenbergstraße 1, D-70569 Stuttgart, Germany*

(Dated: October 20, 2021)

We present a calculation of the spectral properties of a single charge doped at a Cu(3d) site of the Cu-F plane in KCuF₃. The problem is treated by generating the equations of motion for the Green's function by means of subsequent Dyson expansions and solving the resulting set of equations. This method, dubbed the variational approximation (VA), is both very dependable and flexible, since it is a systematic expansion with precise control over elementary physical processes. It allows for deep insight into the underlying physics of polaron formation as well as for inclusion of many physical constraints, such as excluding crossing diagrams and double occupation constraint, which are not included in the Self-Consistent Born Approximation (SCBA). Here we examine the role and importance of such constraints by analyzing various spectral functions obtained in VA and in SCBA.

PACS numbers: 75.25.Dk, 03.65.Ud, 75.10.Lp, 79.60.-i

I. INTRODUCTION

Strongly correlated electron systems with long range ordered ground states exhibit a variety of interesting and complicated phenomena [1–4]. Among the principle problems of interest are those of itinerant charge propagation and its coupling to the polarized background, *e.g.* a hole propagating in an antiferromagnetic CuO₂ plane of a high T_c cuprate superconductor [5]. Such a system is described by the well known t - J model with a SU(2) symmetric Heisenberg Hamiltonian, where fluctuations play a crucial role in the coherent propagation of the charge. In particular, because of the total spin conservation, in the absence of fluctuations the only avenue of coherent charge propagation would be through Trugman loops, a self-healing effective hopping [6].

On the other hand, the orbital models offer a much wider range of charge propagation scenarios. In a system with long range orbital order, the exchange interaction always has a lower symmetry than SU(2), since the fluctuations are suppressed, while the orbital flavor might not necessarily be conserved. Because of that, even if orbital fluctuations are neglected, the charge propagation itself can lead to orbital (de)excitations in the system [7].

Smaller fluctuations of the orbital exchange models mean that orbital systems behave more classically than their spin analogues. For instance, t_{2g} orbital systems exhibit Ising exchange [8], *i.e.*, no fluctuations at all. However, weak hole propagation is still allowed because of three-site processes, which are of the same energy scale as the regular exchange itself. On the other hand, e_g orbital systems, such as KCuF₃, are more complicated, with fluctuations only slightly suppressed due to the orbital symmetries, accompanied by very strong orbital

non-conservation, which is kinetic in nature and governed by the hopping energy scale t [9]. Since this is the dominating interaction of the model, allowing for coherent propagation even if exchange fluctuations and three site terms are neglected, one would expect a quasiparticle (QP) dispersion on the scale of the hopping energy t . The fact that previous research, based on the popular self-consistent Born approximation (SCBA) method, suggested extremely small QP dispersion seems to contradict this intuition. Hence it was suggested that the numerous simplifications required by the SCBA are in fact too restrictive and a more resilient approach is needed to better understand the effective models of e_g systems. Here we make such an attempt via the variational approximation (VA) [10–12], or generating equations of motion for the Green's function.

II. METHODOLOGY

An effective two-dimensional (2D) orbital model of a KCuF₃ ferromagnetic plane can be derived by second order canonical perturbation expansion using σ -bond hopping t along $|3z_\alpha^2 - r^2\rangle$ (where $\alpha = \{x, y, z\}$ is the bond orientation). This derivation, the details of which are too lengthy to be presented here, leads to the following Hamiltonian in the basis of e_g orbitals $\{|z\rangle = |3z^2 - r^2\rangle, |\bar{z}\rangle = |x^2 - y^2\rangle\}$:

$$\begin{aligned} \mathcal{H}_t = & -t \left[\sum_{\langle ij \rangle \| z} d_{iz}^\dagger d_{jz} + \frac{1}{4} \sum_{\langle ij \rangle \| x} (d_{iz}^\dagger - \sqrt{3}d_{i\bar{z}}^\dagger)(d_{jz} - \sqrt{3}d_{j\bar{z}}) \right. \\ & \left. + \frac{1}{4} \sum_{\langle ij \rangle \| y} (d_{iz}^\dagger + \sqrt{3}d_{i\bar{z}}^\dagger)(d_{jz} + \sqrt{3}d_{j\bar{z}}) \right] + \text{H.c.}, \quad (1) \end{aligned}$$

* krzysztof.bieniasz@uj.edu.pl

with orbital exchange interaction

$$\mathcal{H}_J = \frac{J}{2} \sum_{\langle ij \rangle} [T_i^z T_j^z + 3T_i^x T_j^x \mp \sqrt{3}(T_i^x T_j^z + T_i^z T_j^x)], \quad (2)$$

where the operators T^α are analogous to regular spin operators (*i.e.*, 1/2 times the respective Pauli operator), only acting in the e_g orbital space spanned by the $\{|z\rangle, |\bar{z}\rangle\}$ basis.

Henceforth we shall neglect the orbital fluctuations and only keep the Ising part of the exchange Hamiltonian. The reason is that the fluctuations have a smaller amplitude than the leading term of the Hamiltonian [13], while the kinetic energy (1) does not conserve the orbital flavor and so is the source of orbital excitations on a much bigger scale. Furthermore, we will be performing an expansion around a Néel-type ground state, which is inconsistent with keeping the orbital fluctuations.

Since the Ising part of the Hamiltonian is the leading $3T_i^x T_j^x$ term, the basis states are the eigenstates of those operators, *i.e.*, $|\pm\rangle = (|z\rangle \pm |\bar{z}\rangle)/\sqrt{2}$, and so the Hamiltonian needs to be transformed accordingly. Taking into account that the exchange coupling constant J is positive, we can ascertain that the orbital ground state exhibits an alternating orbital (AO) order.

At this point it is useful to decouple the orbital degree of freedom from the fermionic operators by means of slave boson $a^{(\dagger)}$ formalism:

$$d_{i0}^\dagger = f_i^\dagger, \quad d_{i1}^\dagger = f_i^\dagger a_i, \quad (3)$$

where the $\{0, 1\}$ indices denote the ground or excited orbital state, *i.e.*, $|+\rangle$ or $|-\rangle$ depending on the sublattice. After performing those transformations the resulting Hamiltonian takes the final form

$$\mathcal{H}_J = \frac{3}{8} J \sum_{\langle ij \rangle} (1 - \sigma_i^z \sigma_j^z), \quad (4a)$$

$$\mathcal{T} = \frac{t}{4} \sum_{\langle ij \rangle} (f_i^\dagger f_j + \text{H.c.}) = \sum_{\mathbf{k}} \epsilon_{\mathbf{k}} f_{\mathbf{k}}^\dagger f_{\mathbf{k}}, \quad (4b)$$

$$\begin{aligned} \mathcal{V} = & \frac{t}{4} \sum_{i,\delta} \left[(2 + \sqrt{3}e^{i\pi_y \cdot \delta} e^{i\mathbf{Q} \cdot \mathbf{R}_i}) a_i^\dagger + \right. \\ & \left. + (2 - \sqrt{3}e^{i\pi_y \cdot \delta} e^{i\mathbf{Q} \cdot \mathbf{R}_i}) a_{i+\delta}^\dagger + a_i^\dagger a_{i+\delta} \right] f_{i+\delta}^\dagger f_i, \quad (4c) \end{aligned}$$

where $\epsilon_{\mathbf{k}} = t\gamma_{\mathbf{k}}$ is the energy of a free particle, with $\gamma_{\mathbf{k}} = (1/z) \sum_{\delta} e^{i\mathbf{k} \cdot \delta}$. For simplicity, (4a) has been transformed from AO to ferro-orbital state by a rotation on one sublattice, which changes the overall sign of the interaction, hence the $-3/8$ factor in front of J . Note the constant added to the Hamiltonian to put the ground state energy at zero to simplify the calculations. The interaction \mathcal{V} comes from the kinetic Hamiltonian and is a consequence of the orbital flavor non-conservation of the model. The phase factors $\pi_y = (0, \pi)$, $\mathbf{Q} = (\pi, \pi)$ serve to incorporate the model's dependence on direction and delta is the vector pointing to a site's nearest neighbors.

The variational approximation consists in a series of Dyson expansions,

$$\mathcal{G}(\omega) = \mathcal{G}_0(\omega) + \mathcal{G}(\omega) \mathcal{V} \mathcal{G}_0(\omega), \quad (5)$$

to generate the equations of motion for the Green's function, where $\mathcal{H}_0 = \mathcal{T} + \mathcal{H}_J$ corresponds to $\mathcal{G}_0(\omega)$ and \mathcal{V} is given by Eq. (4c). Let us define the Green's function as $G(\mathbf{k}, \omega) \equiv \langle \mathbf{k} | \mathcal{G}(\omega) | \mathbf{k} \rangle$, where $\mathcal{G}(\omega) = (\omega + i\eta - \mathcal{H})^{-1}$ is the resolvent and

$$|\mathbf{k}\rangle \equiv f_{\mathbf{k}}^\dagger |0\rangle = \frac{1}{\sqrt{N}} \sum_i e^{i\mathbf{k} \cdot \mathbf{R}_i} f_i^\dagger |0\rangle, \quad (6)$$

is the free electron Bloch state. The core idea underlying the variational approximation is that the energy cost of an orbiton creation is proportional to J , hence for large J only a small number of orbitons can be created [11].

Since $G_0(\mathbf{k}, \omega)$ is known and diagonal in \mathbf{k} , the key part of the Dyson expansion is evaluating $\mathcal{V}|\mathbf{k}\rangle$, which is done in real space, leading to

$$\begin{aligned} G(\mathbf{k}, \omega) = & \left[1 - \frac{t}{2} \sum_{\delta} F_1(\mathbf{k}, \omega, \delta) + \right. \\ & \left. - \frac{\sqrt{3}t}{4} \sum_{\delta} \bar{F}_1(\mathbf{k}, \omega, \delta) e^{i\pi_y \cdot \delta} \right] G_0(\mathbf{k}, \omega - 4J'), \quad (7) \end{aligned}$$

where $J' = \frac{3}{8}J$ and the generalized Green's functions

$$F_1(\mathbf{k}, \omega, \delta) = \langle \mathbf{k} | \mathcal{G}(\omega) \frac{1}{\sqrt{N}} \sum_i e^{i\mathbf{k} \cdot \mathbf{R}_i} f_{i+\delta}^\dagger a_i^\dagger |0\rangle, \quad (8)$$

$$\bar{F}_1(\mathbf{k}, \omega, \delta) = \langle \mathbf{k} | \mathcal{G}(\omega) \frac{1}{\sqrt{N}} \sum_i e^{i(\mathbf{k} + \mathbf{Q}) \cdot \mathbf{R}_i} f_{i+\delta}^\dagger a_i^\dagger |0\rangle. \quad (9)$$

These functions are unknown and need to be calculated by further Dyson expansions which, after applying \mathcal{V} to the $f_{i+\delta}^\dagger a_i^\dagger |0\rangle$ state, generate other Green's functions, such as $G(*, *)$, $F_1(*, *, *)$ and the 2-orbiton functions

$$F_2(\mathbf{k}, \omega, \delta, \epsilon) = \langle \mathbf{k} | \mathcal{G}(\omega) \frac{1}{\sqrt{N}} \sum_i e^{i\mathbf{k} \cdot \mathbf{R}_i} f_{i+\delta+\epsilon}^\dagger a_{i+\delta}^\dagger a_i^\dagger |0\rangle, \quad (10)$$

which also need to be expanded further. This process could be continued indefinitely, so at some point the equations have to be cut by disallowing the creation of any further orbitons in the system, hence it is controlled by the number of orbital excitations.

Once the system has more than one orbiton, there are numerous ways to de-excite it, namely at each step an orbiton can be removed from either end of the string. In particular, destroying an orbiton other than the one created last is a process analogous to the crossing-diagrams excluded in SCBA. Here we try to establish the importance of such processes by comparing the Green's functions which include or exclude them in the 2-orbiton regime.

After the first orbiton is added, certain constraints have to be imposed on the electron's movement, namely: (*i*)

the electron cannot occupy the same site as the orbiton, and (ii) in the case where the electron is on a site adjacent to the orbiton the \mathcal{H}_J energy increase is $10J'$, compared to the regular energy $12J'$ when the particles are far apart. Because of this, the translational invariance is broken, so that \mathbf{k} is no longer a good quantum number. Therefore, at higher levels of the expansion one has to calculate real space Green's functions while including the above constraints, which is added as a term to the Hamiltonian \mathcal{H}_0 to cancel the corresponding processes:

$$\mathcal{V}_1 = -\frac{t}{4} \sum_{\epsilon} (f_i^\dagger f_{i+\epsilon} + \text{H.c.}) - 2J' \sum_{\epsilon} n_{i+\epsilon}, \quad (11)$$

where i is the location of the orbiton and $n_{i+\epsilon}$ is the electron number operator. The constrained non-interacting Green's function is then calculated from the non-constrained one similarly, by Dyson expansion

$$\mathcal{G}_1(\omega) = [1 + \mathcal{G}_1(\omega)\mathcal{V}_1]\mathcal{G}_0(\omega), \quad (12)$$

which leads to a matrix equation, describing propagations between the orbiton's neighboring sites

$$\mathbb{G}_1^{\gamma\delta} = \mathbb{G}_0^{\gamma\epsilon} [\mathbb{I}^{\delta\epsilon} + \frac{t}{4}\mathbb{G}_0^{\delta 0} + 2J'\mathbb{G}_0^{\delta\epsilon}]^{-1}, \quad (13)$$

where the Greek indices denote the orbiton's neighboring sites, so the matrix element $\mathbb{G}_1^{\gamma\delta} = G_1(\gamma, \delta, \omega)$ is the constrained Green's function describing the $|i+\delta\rangle \rightarrow |i+\gamma\rangle$ propagation in real space. A similar equation is found for the case of two or more orbitons, only the indices run over all the neighboring sites of the orbiton string.

Once the equations of motion for the Green's function are generated and cut at the desired level (in this work at two orbitons), one is left with a set of equations for various Green's functions. In principle the system can be solved for all of them, but usually we are only interested in the normal Green's function $G(k, \omega)$. However, what is usually plotted is the normalized spectral function

$$A(\mathbf{k}, \omega) = -\frac{1}{\pi} \Im[G(\mathbf{k}, \omega)], \quad (14)$$

which has the interpretation of the quasiparticle density of states. Furthermore, here we plot $\tanh[A(k, \omega)]$, which amplifies the low amplitude part of the spectra, while treating the large amplitudes almost uniformly by mapping them into values close to 1.

III. RESULTS AND DISCUSSION

In Fig. 1 the calculated spectral functions are shown in a nonlinear tanh-scale to emphasize the low amplitude features of the spectral functions. Panel (a) shows the full Green's function, including the crossing diagrams and the translational constraints, while panels (b)–(d) focus on the difference functions when constraints are neglected, see below.

The huge advantage of the VA is that it is an analytical method with precise control of the states spanning the Hilbert space. When performing the expansion and evaluating the interaction, one can easily include or omit processes according to their importance or likelihood of occurrence. For instance, if the system, after creating multiple bosons, starts removing them in an order reverse to the order of creation, then it is a non-crossing process, because the bosonic lines of its Feynman diagram can never cross. Any other sequence of boson removals leads to crossing diagrams, and the relative number of such processes is the bigger the more bosons there are in the system. However, their importance can be hard to ascertain as it mostly depends on the interaction vertex and the boson energy. Knowing the significance of the crossing-diagrams is very important for using methods like the SCBA, since it is an approximation that by its very nature includes only non-crossing diagrams, while adding other processes can be very tricky. However, since VA makes it easy to turn those processes on or off, it is a good method to check their role, even if only within a low expansion order.

On the other hand, SCBA, being a Fourier space expansion, requires full translational invariance. However, as already explained, this is broken once there are bosons in the system. Therefore, SCBA simply ignores that, assuming that for a big system with a small number of bosons the lattice is almost fully translational invariant. However, polaronic physics is strongly local, with all the interactions happening in the vicinity of the boson. Therefore, in general the translational constraints are expected to play a crucial role. Unfortunately, SCBA cannot include those effects at all, while VA does it exactly and fully. In this paper we use the VA [10] to examine the importance of the two effects described above. To do so, we calculate Green's functions including both of the effects, excluding either of them, or excluding both.

Panel (b) shows the difference function for the case without cross-diagrams, but including translational constraints. Somewhat surprisingly, we see that at the lowest order of expansion the cross-diagrams play a very small, almost negligible role, with maximal values of amplitude change at around 5%. The qualitative change of the spectrum is also very subtle, with only a tiny transfer of weight at Γ and M points and a small reduction of bandwidth (indicated by a pair of parallel red-blue lines in the function, which mean that the reference maximum of panel (a) has to move away from the blue line and towards the red line).

On the other hand, the effect of the translational constraints is very strong. Panel (c) shows that neglecting this effect causes the QPs to gain additional energy, by shifting the whole spectrum upwards. This is especially dramatic for the excited state in the upper part of the spectrum where the shift is around $0.13t$ and the amplitude is very big, while in the ground state at the bottom the effect is somewhat smaller, with a shift of $0.06t$ and the amplitude change of around 3%. This however is still

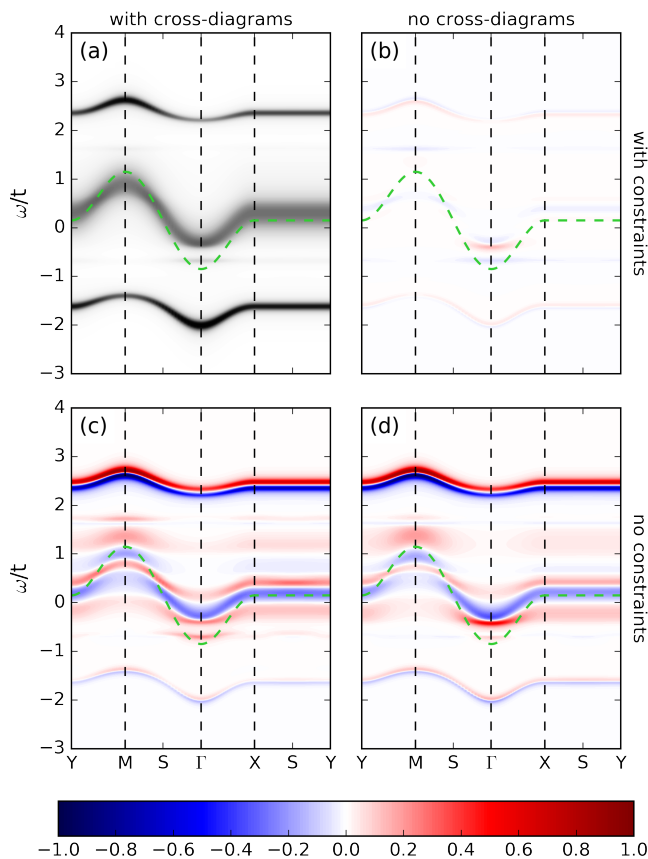


FIG. 1. Spectral functions $A(\mathbf{k}, \omega)$ for $J/t = 0.1$: (a) the full function, including cross-diagrams and constraints, (b) difference for the case without cross-diagrams, (c) difference for the case without constraints, (d) difference for the case without both effects. The dashed green line indicates the free electron dispersion $\omega = \epsilon_k + 4J'$ for reference. The colorbar refers only to panels (b)–(d). Note the tanh-scale.

bigger than the effect of cross-diagrams. In the incoherent part of the spectrum in the middle, the influence of the constraints is quite strong but qualitatively complicated. The exclusion of constraints seems to narrow the width of the pseudo-band visible in the middle of panel (a) on one hand, and tend to split the band into two around $\omega = 0$

on the other, but not enough to separate them completely. This has the effect that although the spectrum in the middle becomes more coherent, it appears even less so because the various bands blend together. This in principle is in accordance with SCBA, which shows a broad incoherent continuum, with a barely discernible ladder of low amplitude states. However, this effect does not seem to account for the whole difference, since the two results still differ quite substantially.

Finally, panel (d) shows the results when both cross-diagrams and constraints are turned off. Since the two effects are completely independent and do not interfere with each other, it is no surprise that their combined effect does not differ much from those effects treated separately. In particular, since the cross-diagram effects are so small, it is clear that the results in panel (d) are nearly identical to those in panel (c). A close inspection might reveal that some of the features are more pronounced, especially where the two effects would combine positively, such as in the ground state or in the incoherent part around the Γ point. However, qualitatively the picture remains mostly the same.

In conclusion, we have shown, using a highly accurate and primarily analytical method, the effects of two most important approximations employed by the SCBA, which is a standard method widely used in polaronic physics. We have shown that within our e_g orbital model the effects of cross-diagrams is very small and can mostly be neglected. However, due to the highly local nature of the polaronic QPs, the translational constraint effects are very important and cannot conceivably be neglected. Furthermore, they can to some extent explain the difference between SCBA and VA, although not fully. Since there is no way to include those constraints in SCBA, that method should be used with caution.

ACKNOWLEDGMENTS

We thank Krzysztof Wohlfeld for insightful discussions. We kindly acknowledge support by UBC Quantum Matter Institute, by Natural Sciences and Engineering Research Council of Canada (NSERC), and by Narodowe Centrum Nauki (NCN) under Projects No. 2012/04/A/ST3/00331 and 2015/16/T/ST3/00503.

- [1] G. Khaliullin, *Prog. Theor. Phys. Suppl.* **160**, 155 (2005). <http://dx.doi.org/10.1143/PTPS.160.155>
- [2] A.J.W. Reitsma, L.F. Feiner, A.M. Oleś, *New J. Phys.* **7**, 121 (2005). <http://dx.doi.org/10.1088/1367-2630/7/1/121>
- [3] P. Wróbel, A.M. Oleś, *Phys. Rev. Lett.* **104**, 206401 (2010). <http://dx.doi.org/10.1103/PhysRevLett.104.206401>
- [4] W. Brzezicki, A.M. Oleś, M. Cuoco, *Phys. Rev. X* **5**, 011037 (2015).

- [5] G. Martínez, P. Horsch, *Phys. Rev. B* **44**, 317 (1991). <http://dx.doi.org/10.1103/PhysRevB.44.317>
- [6] S.A. Trugman, *Phys. Rev. B* **37**, 1597 (1988). <http://dx.doi.org/10.1103/PhysRevB.37.1597>
- [7] J. van den Brink, P. Horsch, A.M. Oleś, *Phys. Rev. Lett.* **85**, 5174 (2000). <http://dx.doi.org/10.1103/PhysRevLett.85.5174>
- [8] M. Daghofer, K. Wohlfeld, A.M. Oleś, E. Arrighoni, P. Horsch, *Phys. Rev. Lett.* **100**, 066403 (2008). <http://dx.doi.org/10.1103/PhysRevX.5.011037>

- <http://dx.doi.org/10.1103/PhysRevLett.100.066403>
- [9] L.F. Feiner, A.M. Oleś, *Phys. Rev. B* **71**, 144422 (2005).
<http://dx.doi.org/10.1103/PhysRevB.72.144422>
- [10] M. Berciu, H. Fehske, *Phys. Rev. B* **84**, 165104 (2011).
<http://dx.doi.org/10.1103/PhysRevB.84.165104>
- [11] F. Trouselet, M. Berciu, A.M. Oleś, P. Horsch, *Phys. Rev. Lett.* **111**, 037205 (2013).
<http://dx.doi.org/10.1103/PhysRevLett.111.037205>
- [12] H. Ebrahimnejad, G.A. Sawatzky, M. Berciu, *Nature Physics* **10**, 951–955 (2014).
<http://dx.doi.org/10.1038/nphys3130>
- [13] L. Cincio, J. Dziarmaga, A.M. Oleś, *Phys. Rev. B* **82**, 104416 (2010).
<http://dx.doi.org/10.1103/PhysRevB.82.104416>